Nonlinear response of pile-soil system under harmonic lateral loading

Hamdi, S., Allani, M. & Holeyman, A.
Université Catholique de Louvain, Belgium

Keywords: pile interaction, nonlinear behavior, lateral loading

ABSTRACT: This paper presents a new model to analyze the nonlinear interaction between a vertical cylindrical pile subjected to lateral harmonic loading and its embedment soil. The pile toe is either pinned or clamped to idealize its support on bedrock. The soil mass is decomposed into an inner soil zone around the pile where soil nonlinearity is portrayed by a hyperbolic model and a linearly elastic outer soil zone. A numerical solution is obtained using the finite difference method. The results obtained by the suggested approach are then compared with those derived from an analytical approach developed by Nogami and Novak (1977).

1 INTRODUCTION

Pile Foundations are used for a variety of civil and geotechnical engineering purposes. The forces on these structures consist of vertical loads due to self weight of the superstructure and lateral loads. The latter can be produced by machines, wind, earthquake, ships, wave loads and result in eccentric loading. Numerous studies have been performed to determine of the response of a soil-pile system to harmonic lateral loading. In fact, dynamic soil-pile interaction under lateral loading is a very complex problem and linear elastic behavior of soils has been considered in earlier studies to simplify the problem. Some linear analytical studies have been proposed by a. o. Novak and Nogami (1977). Many other researchers including El Naggar and Novak (1995), Badoni and Markis (1995), Chau and Yang (2005) have investigated the dynamic response of a single pile assuming nonlinear behavior of soil.

In this paper, on the one hand, the analytical solution suggested by Novak and Nogami (assuming a linear elastic behavior of the soil) is examined using a parametric study in order to investigate the impact of some parameters on the response of the soil-pile system. On the other hand, a numerical approach based on a finite difference method is developed. The suggested approach aims to account for the non-linear behavior of the soil without enduring too high a numerical penalty.

2 ANALYTICAL APPROACHES FOR PLANE STRAIN LINEAR BEHAVIOR

2.1 Problem statement

This paper attempts to determine the response of the soil-pile system when harmonic loading is applied at the pile head (Fig. 1). The pile is supposed to be elastic, vertical and cylindrical. The pile is either pinned or clamped at its toe to portray its support on bedrock. It can be noted that the imposed harmonic displacement is aligned according to $\theta=0$ where θ is the azimuthal angle.

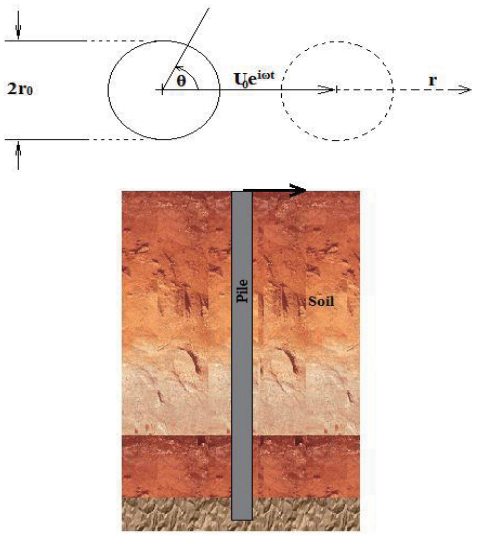

Figure 1. Soil-pile systm.

Table 1 provides a list of the problem parameters, their symbols and units.

Table1. Pile, soil and loading parameters.

Symbol		Description	Unit	Value
Pile	r_0	Pile radius	[m]	0.3
	H	Pile length	[m]	12
	I	Pile's moment of inertia	[m^4]	0.0064
	E	Pile's Young modulus	[psi]	$3.5\ 10^6$
	ρ_p	density	[$kg.m^{-3}$]	3600
Soil	G	Representative shear modulus	[MPa]	-
	G_{max}	Maximum shear Modulus	[MPa]	8
	γ_r	Reference shear strain	[.]	$2.25\ 10^{-4}$
	D	Hysteretic damping	[%]	-
	ν	Poisson 's ratio	[.]	0.4
	ρ	Soil density	[$kg.m^{-3}$]	1800
Loading	ω	Angular frequency	[$rad.s^{-1}$]	40
	u_0	Oscillation amplitude	[m]	$r_0/1000$

2.2 *Unit slice : Novak et al (1978)*

The response of an embedded pile to dynamic lateral loads can be predicted if the reactions of the soil to the motion of the pile can be assessed. We summarize below key results of Novak et al (1978) based on analytical approaches. These authors defined soil reactions to harmonic motion of a cylindrical body embedded in a linear elastic medium limited to cases that can viewed as plane strain. Such a situation arises when an infinitely rigid long cylinder embedded in an infinite medium undergoes uniform transverse displacements or rotates about its axis. In that case, no strain develops across the plane perpendicular to the axis, allowing consideration of a unit thickness of the medium. The assumptions adopted in this approach are: the soil medium is infinite, homogeneous, isotropic and viscoelastic with frequency independent material damping (hysteretic damping). The embedded cylinder is massless and infinitely long. The soil-pile system is subjected to a uniform lateral displacement: $u_0=U_0e^{i\omega t}$ (Fig. 2).

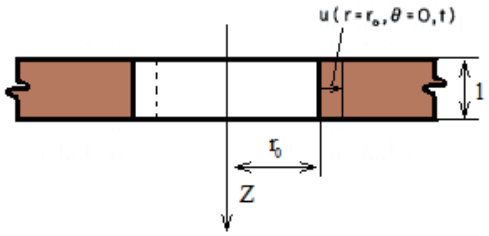

Figure 2. Plane strain (horizontal vibration).

The hysteretic damping ratios associated with the volumetric and shear strains respectively can be written as $D_v=\lambda'/\lambda$ and $D_s=G'/G$ where $G^*=G+iG'$ and $\lambda^*=\lambda+i\lambda'$ are the complex Lamé's constants describing the soil viscoelasticity.

The reaction of the soil per pile unit length can be modeled by a spring of stiffness k_u. The complex horizontal stiffness or impedance (k_u) per unit length of the cylinder represents the soil reaction to a harmonic displacement of unit amplitude:

$$k_u = \pi G a_0^2 T = G(S_{u1} + iS_{u2}) \quad (1)$$

$$T = -\frac{4K_1(b_0^*)K_1(a_0^*) + a_0^*K_1(b_0^*)K_0(a_0^*) + b_0^*K_0(b_0^*)K_1(a_0^*)}{b_0^*K_0(b_0^*)K_1(a_0^*) + a_0^*K_1(b_0^*)K_0(a_0^*) + a_0^*b_0^*K_0(b_0^*)K_0(a_0^*)} \quad (2)$$

where :

$$a_0 = \frac{r_0\omega}{V_s}, a_0^* = \frac{ia_0}{\sqrt{1+1D_s}}, b_0^* = \frac{a_0 i}{\eta\sqrt{1+iD_1}}, D_1 = \frac{\lambda'+2G'}{\lambda+2G}$$

denoting the longitudinal and shear wave velocities in an elastic medium and their ratio:

$$V_L = \sqrt{\frac{(\lambda+2G)}{\rho}}, V_S = \sqrt{\frac{G}{\rho}}, \eta = \frac{V_L}{V_S} = \sqrt{\frac{2(1-\nu)}{1-2\nu}}$$

Figure 3 represents the S_{u1} and S_{u2} components of the lateral pile impedance according to Novak et al's Equations (1) and (2) as functions of the adimensional frequency a_0 for differents values of the hysteretic damping D_s (=D_v).

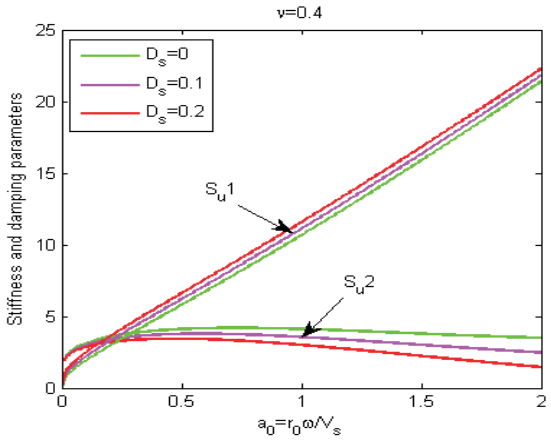

Figure 3. Stiffness and damping parameters for unit slice.

2.3 Thick soil layer (Nogami and Novak 1977)

The reaction of a soil layer to the steady state horizontal vibration of an elastic pile has been theoretically investigated by Nogami and Novak (1977). The pile is assumed to be vertical and of circular cross-section (Figure 1). The soil is modeled as a linear elastic layer with hysteretic material damping. The assumptions adopted in this approach are: the bottom of the layer is fixed, the vertical displacements associated with horizontal vibration are negligibly small and the motion is harmonic. The equations of the viscoelastic layer undergoing harmonic motion can be written in the following classical form:

$$(\lambda+2G)\frac{\partial\Delta}{\partial r}-\frac{2G}{r}\frac{\partial w_z}{\partial\theta}=\rho\frac{\partial^2 u}{\partial t^2}-G\frac{\partial^2 u}{\partial z^2} \quad (3)$$

$$(\lambda+2G)\frac{\partial\Delta}{r\partial\theta}+2G\frac{\partial w_z}{\partial r}=\rho\frac{\partial^2 v}{\partial t^2}-G\frac{\partial^2 v}{\partial z^2} \quad (4)$$

where u and v are respectively the radial and the ortho-radial displacements and:

$$\Delta=\frac{1}{r}\frac{\partial(ru)}{\partial r}+\frac{1}{r}\frac{\partial v}{\partial\theta} \quad (5)$$

$$w_z=\frac{1}{2}\left(\frac{1}{r}\frac{\partial(rv)}{\partial r}-\frac{1}{r}\frac{\partial u}{\partial\theta}\right) \quad (6)$$

According to Novak and Nogami's analytical development, the solution can be expressed in terms of displacement as Bessel series.

$$u(r,\theta,z)=\cos(\theta)\sum_{n=1}^{\infty}\sin(h_n z)\left\{-A_n\left[\frac{1}{r}K_1(q_n r)+q_n K_0(q_n r)\right]+B_n\frac{1}{r}K_1(s_n r)\right\} \quad (7)$$

$$v(r,\theta,z)=\sin(\theta)\sum_{n=1}^{\infty}\sin(h_n z)\left\{-A_n\frac{1}{r}K_1(q_n r)+B_n\left[\frac{1}{r}K_1(s_n r)+s_n K_0(s_n r)\right]\right\} \quad (8)$$

where K_0 and K_1 are the modified Bessel functions of the second kind, of the 0th and first order respectively, A_n and B_n are integration constants determined from the boundary conditions, and:

$$h_n=\frac{\pi}{2H}(2n-1) \quad (9)$$

$$q_n^{\,2}=\frac{(1+iD_s)h_n^{\,2}-\left(\frac{\omega}{V_s}\right)^2}{\eta^2+i[(\eta^2-2)D_v+2D_s]} \quad (10)$$

$$s_n^{\,2}=\frac{(1+iD_s)h_n^{\,2}-\left(\frac{\omega}{V_s}\right)^2}{1+iD_s} \quad (11)$$

2.4 Response of the pile to a harmonic loading

In this section are reviewed the mechanical characteristics of the pile in order to assess the response of the soil-pile system to a harmonic loading in terms of local deformation, tilt, shear force, and bending moment of the pile. The pile head is subjected to a harmonic lateral displacement $u_0=U_0e^{i\omega t}$, as shown in Figure 1.

The governing equation of the pile motion is:

$$E_p I\frac{\partial^4(Ue^{i\omega t})}{\partial z^4}+m\frac{\partial^2(Ue^{i\omega t})}{\partial t^2}=-p(z)e^{i\omega t} \quad (12)$$

In which, E_pI is the bending moment of the pile, m is the mass of the pile per unit length, and p(z) is the amplitude of the soil reaction to the motion of the pile:

$$p(z)=-\int_0^{2\pi}\left[\sigma_r(r_0)\cos(\theta)-\tau_{r\theta}(r_0)\sin(\theta)\right]r_0 d\theta \quad (13)$$

The value of p(z) can be obtained based on the analytical results from Section 2.3. Then the amplitude of the angle of rotation (tilt ϕ), of the bending moment M, and of the shear force S are obtained from the standard relationships:

$$\phi(z)=\frac{\partial u}{\partial z} \quad (14)$$

$$M(z)=E_p I\frac{\partial^2 u}{\partial z^2} \quad (15)$$

$$S(z)=E_p I\frac{\partial^3 u}{\partial z^3} \quad (16)$$

2.5 Parametric study

Figures 4, 5 and 6 present the results of a parametric study allowing the evaluation of the impact of the pile slenderness, Poisson's ratio, and hysteretic damping, respectively, on both real and imaginary parts of the shear force S at the pile's head in response to the imposed harmonic displacement.

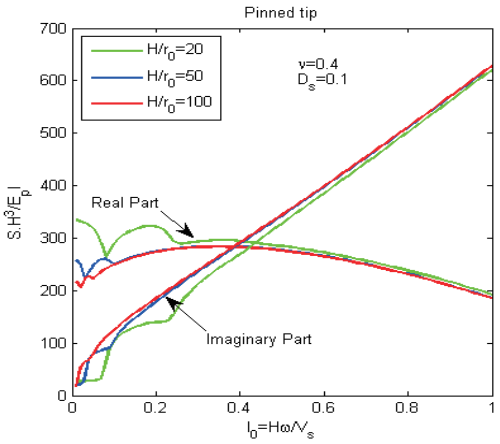

Figure 4. Head stiffness: influence of pile slenderness.

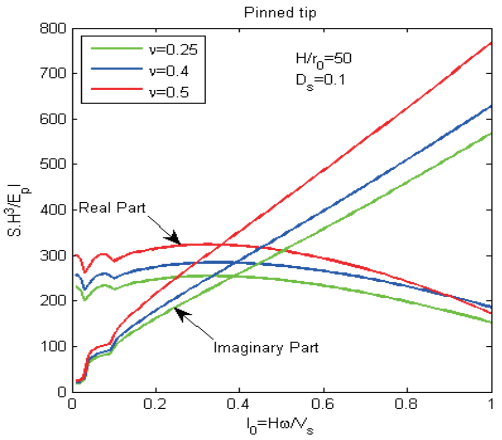

Figure 5. Head stiffness: influence of Poisson's ratio.

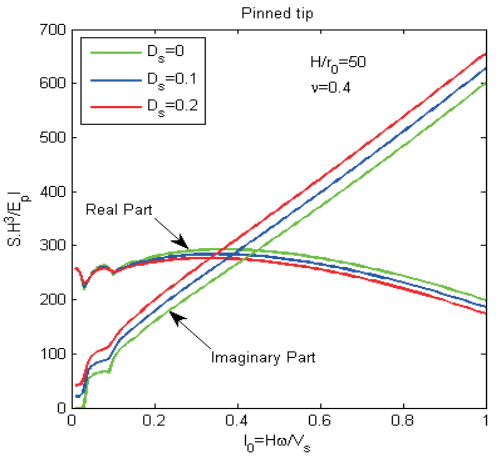

Figure 6. Head stiffness: influence of hysteretic damping.

Comparing Figures 4 through 6 to Figure 3 (unit slice modeling), it can noted that both real and imaginary parts of the head stiffness have the similar shapes. One significant difference between the two problems is the emergence of cutoff frequencies in the thick soil layer modeling.

3 NUMERICAL APPROACH FOR SOIL NONLINEAR MODELING

3.1 Soil stiffness degradation: Kondner modeling

The hyperbolic model of Kondner will be introduced in the numerical approach to express the degradation of soil shear stiffness as strain increases. This hyperbolic model expresses the secant shear modulus as a function of the shear deformation $\gamma_{r\theta}$ as follows:

$$G = G_{\max} \frac{\gamma_r}{\gamma_r + \gamma_{r\theta}} \tag{17}$$

$$\gamma_r = \frac{\tau_{\max}}{G_{\max}} \tag{18}$$

$$\xi = \frac{2}{\pi}\left[2\frac{\gamma_r}{\gamma_c^2}(\gamma_r + \gamma_c)Log\left(\frac{\gamma_r}{\gamma_c + \gamma_r}\right) + 2\frac{\gamma_r}{\gamma_c} + 1\right] \tag{19}$$

where γ_r, γ_c, τ_{max}, and ξ are respectively, the reference shear strain, the amplitude of the shear strain, the maximum shear stress, and the hysteretic damping.

Figures 7 and 8 present, respectively, the resulting variation of the secant shear modulus and the hysteretic damping with the shear strain.

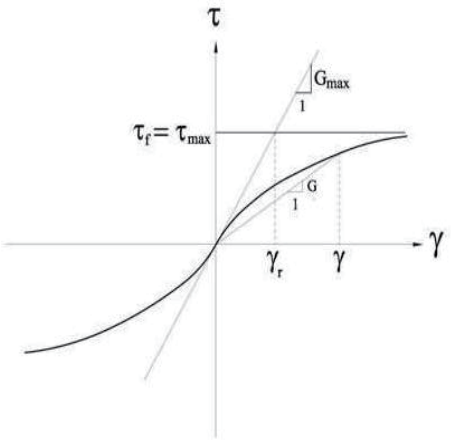

Figure 7. Stress strain law of (Kondner, 1963).

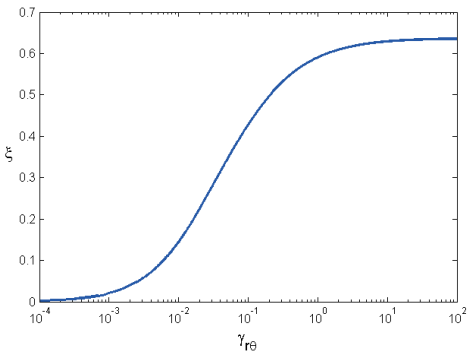

Figure 8. Hysteretic damping variation with shear strain.

3.2 Numerical modeling: finite difference method

3.2.1 Partial differential equations

The degradation of the shear modulus according to Equation (17) results in the shear modulus no longer remaining constant: it ends up varying as a function of the radial distance from the axis of the pile: G=G(γ). As a result, the partial differential equations describing the dynamic equilibrium can be written as follows:

$$\left[\lambda(r)+2G(r)\right]\frac{\partial}{\partial r}\nabla^2\varphi-\frac{1}{r}G(r)\frac{\partial}{\partial\theta}\nabla^2\psi=-\left[\rho\omega^2-G(r)\frac{\partial^2}{\partial z^2}\right]\left(\frac{\partial\varphi}{\partial r}+\frac{1}{r}\frac{\partial\psi}{\partial\theta}\right)+\left\{-2\frac{\partial G(r)}{\partial r}\left(\frac{\partial^2\varphi}{\partial r^2}-\frac{1}{r^2}\frac{\partial\psi}{\partial\theta}+\frac{1}{r}\frac{\partial^2\psi}{\partial r\partial\theta}\right)\right\} \quad (20)$$

$$\left[\lambda(r)+2G(r)\right]\frac{\partial}{r\partial\theta}\nabla^2\varphi-G(r)\frac{\partial}{\partial r}\nabla^2\psi=-\left[\rho\omega^2-G(r)\frac{\partial^2}{\partial z^2}\right]\left(\frac{\partial\varphi}{r\partial\theta}-\frac{\partial\psi}{\partial r}\right)+\left\{-\frac{\partial G(r)}{\partial r}\left(\frac{2}{r^2}\frac{\partial^2\varphi}{\partial\theta^2}+\frac{2}{r}\frac{\partial^2\psi}{\partial r\partial\theta}+\nabla^2\psi-\frac{\partial^2\psi}{\partial^2 r}\right)\right\} \quad (21)$$

3.2.2 Boundary conditions

The soil mass is decomposed into a nonlinear inner soil zone around the pile where the soil nonlinearity is handled via of Kondner's hyperbolic model and a linearly elastic outer soil zone. Only the inner zone is discretized to obtain a numerical solution using the finite difference method. The behavior of the outer zone is handled by the introduction of Novak et al's impedance expressions (Equations (1) and (2)) at the outer boundary of the inner soil zone.

The boundary conditions are as follows: pile displaced at the head, clamped or pinned at the toe, as shown in Fig. 9.

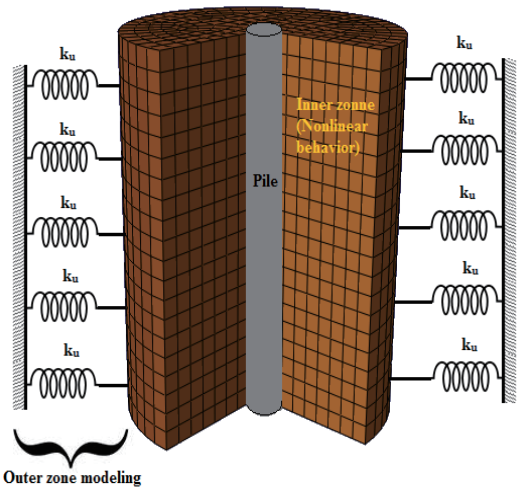

Figure 9. Inner and outer zone modeling.

3.2.3 Finite difference method formulation

Using the problem natural cylindrical coordinates system (Fig. 10), displacements and its derivatives at a node having (i, j, k) as radial, azimuthal and axial coordinates numbers are approximated using the displacements of the surrounding nodes.

The derivatives at a node (i, j, k) are approximated by the following expressions:

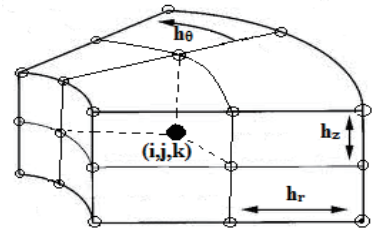

Figure 10. Finite difference method.

3.2.4 Algorithm

The numerical method is implemented in an iterative algorithm schematized in Fig. 11. This algorithm takes into accounts the nonlinear behavior of the soil

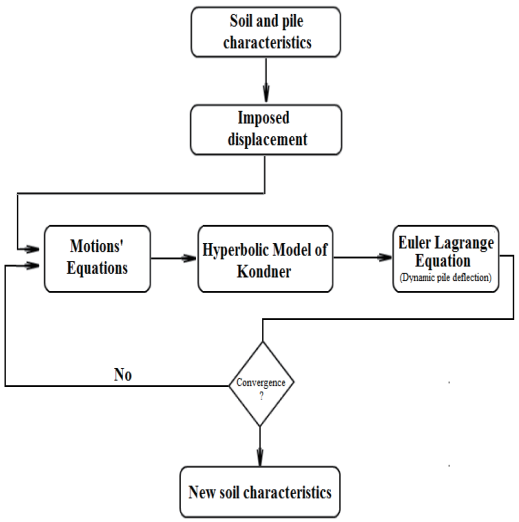

Figure 11. Algorithm.

4 RESULTS

4.1 Comparison with the linear analytical method

A comparative study is performed in order to confirm the results of the numerical approach by reference to those given by Novak and Nogami's analytical approach while applying a small amplitude of vibration ($U_0=r_0/10^6$).

Figures 12 and 13 present the results of the comparative study in terms amplitude of radial stress for two cases: static and dynamic (ω=40 rad.s^{-1}).

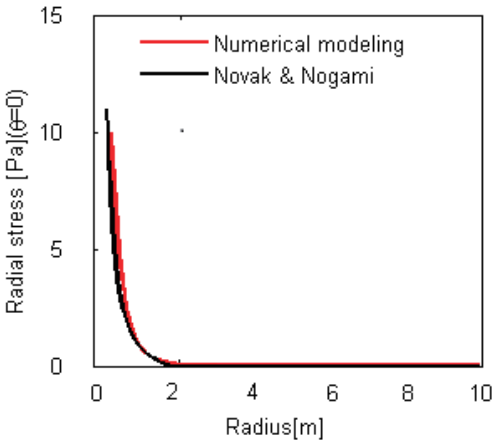

Figure 12. Radial stress attenuation along θ=0 direction (static case).

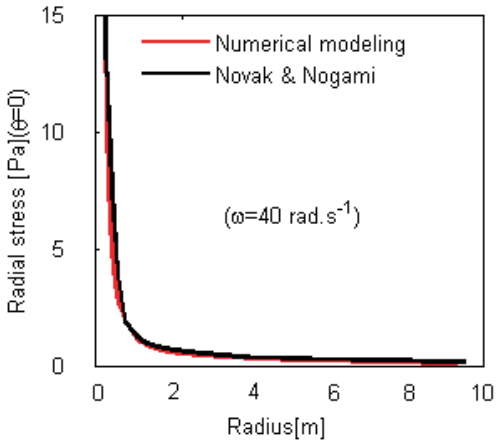

Figure 13. Radial stress attenuation along θ=0 direction (dynamic case).

According to this comparison, the proposed numerical approach gives results similar to Novak et Nogami's analytical approach, in the case of small amplitudes of vibration.

4.2 Simulations highlighting non linear behavior

4.2.1 Hysteretic damping

Results showing parameters distributions will be presented within two radial planes that will be labeled as follows:
- Movement radial plane, when the plane is parallel to the imposed displacement (θ=0).
- Movement orthoradial plane, when the plane is orthogonal to the imposed displacement (θ=π/2).

Figures 14 and 15 represent the distribution of the hysteretic damping in the movement radial plane and the movement orthoradial plane respectively, when the pile's head is subjected to a harmonic displacement of amplitude $U_0=r_0/1000$ (refer to Table 1 for other parameters)

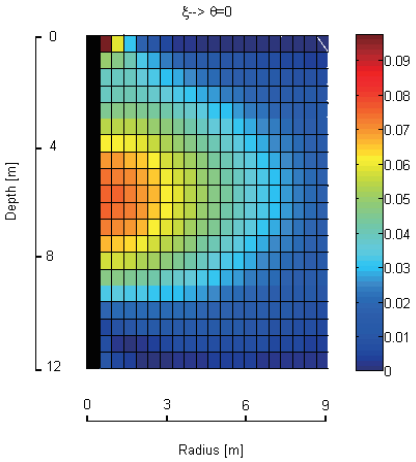

Figure 14. Hysteretic damping distribution (θ=0).

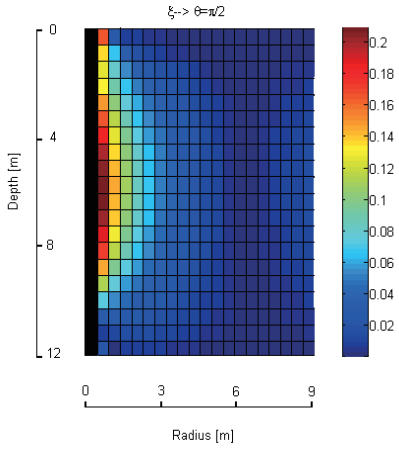

Figure 15. Hysteretic damping distribution (θ=π/2).

4.2.2 Shear modulus

Figures 16 and 17 represent the distribution of the shear modulus in the movement radial plane and the movement orthoradial plane respectively, when the pile's head is subjected to a harmonic displacement.

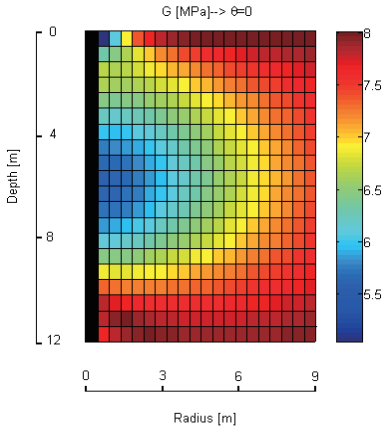

Figure 16. Shear modulus distribution (θ=0).

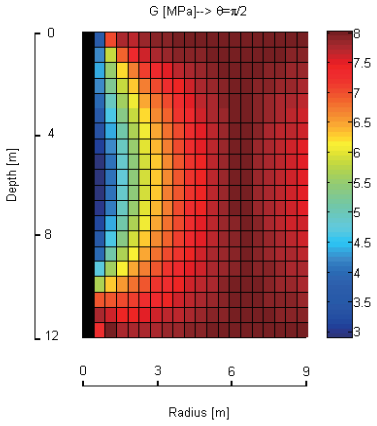

Figure 17. Shear modulus distribution (θ=π/2).

The lowest values of shear modulus are located at the direction (θ=π/2) since the highest values of the shear strain are located along this direction.

4.2.3 Stress field

Figures 18, 19, and 20 represent, respectively, the distribution of the axial vertical stress, the radial stress, and the orthoradial stress in the movement orthoradial plane.

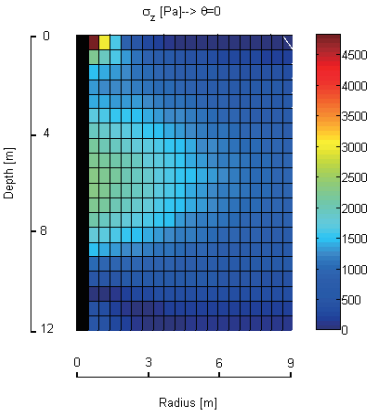

Figure 18. Axial vertical stress distribution (θ=0)

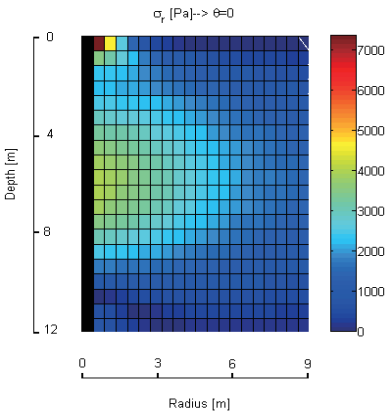

Figure 19. Radial stress distribution (θ=0).

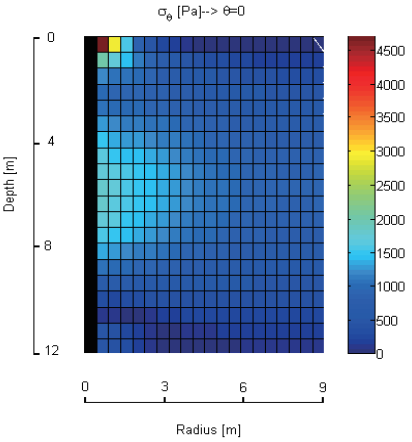

Figure 20. Ortho-radial stress distribution (θ=0).

5 CONCLUSION.

The nonlinear response of the soil-pile system under lateral harmonic loading can be simulated using the suggested numerical approach based on a finite difference method, and allows us to draw some conclusions.

The numerical results have been compared with the analytical results of Novak and Nogami for the case of low amplitudes of vibration. This comparison shows a good match between the two approaches.

The nonlinear behavior of soil should be considered in the soil-pile interaction study because it can significantly affect the stiffness and damping of the soil-pile system, especially for the case of large deformations.

REFERENCES

Badoni. D and Makris. N. (1996). "Nonlinear response of single piles under lateral inertial and seismic loads", Soil Dynamic and Earthquake Engineering, pp.29-43.

Chau, K. T and Yang, X. (2005). "Nonlinear interaction of soil-pile in horizontal vibration", Journal of Engineering Mechanics, pp.847-858.

El Naggar. M. H and Novak. M. (1996). "Nonlinear analysis for dynamic lateral pile response", Soil Dynamic and Earthquake Engineering, pp.-244.

Kondner, R. L. (1963). "Hyperbolic stress-strain response: cohesive soils", Journal of the Soil Mechanics and Foundations Division, ASCE, vol. 89, pp.115-143.

Nogami. T and Novak. M. (1977). "Resistance of soil to a vibrating pile", Int. J. Earthquake Engineering and Structural Dynamics, Vol. 5, pp.249-261.

Novak. M, Nogami. T and Aboul-Ella. F. (1978). "Dynamic soil reactions for plane strain case", Technical Notes, pp.953-959.

Novak. M and Nogami. T. (1977). "Soil-pile interaction in horizontal vibration", Earthquake Engineering and Structural Dynamics, Vol. 5, pp.263-281.